The following text was not accepted as a "comment" by Geochimica et Cosmochimica Acta because of its length. However, it illustrates in more detail the points of disagreement, which were not sufficiently addressed in the "reply" of Steele-MacInnis and Bodnar.

Comment

Comment on "Effect of the vapor phase on the salinity of halite-bearing aqueous fluid inclusions estimated from the halite dissolution temperature", by M. Steele-MacInnis and R.J. Bodnar

Ronald J. Bakker

Department of Applied Geosciences and Geophysics, Resource Mineralogy, University of Leoben, Peter-Tunner-Str. 5, A-8700 Leoben, Austria

Abstract

Recently Steele-MacInnis and Bodnar reported an experimental study on the estimation of the salinity of halite bearing fluid inclusions from dissolution temperatures of halite crystals, in the presence and absence of a vapour phase (Steele-MacInnis, M., Bodnar, R .J., 2013, *Geochimica et Cosmochimica Acta* **115**, 205-216). The authors present new purely empirical equations to calculate fluid inclusion bulk salinity, which is mainly determined by dissolution temperature of halite (*SLV*→*LV*) with a minor correction due to presence of a vapour phase at higher temperatures, similar to the study of Bakker (2012a, *Central European Journal of Geoscience* **4**, 238-245). The experimental approach in their work is inappropriate, the mathematical modelling is insufficient and partly erroneous, and comparison with the model from Bakker (2012a) is inconsistent and imprecise.

1. INTRODUCTION

In fluid inclusion studies, the salinity of aqueous fluids is estimated directly from dissolution temperatures of ice, salt-hydrates, and salts (e.g. Shepherd et al., 1985). This method includes a variety of disregarded assumptions that may play an important role in the estimation of the fluid properties in inclusions. First, dissolution temperature of ice and salt-hydrates below 0 ˚C and salt above 0 ˚C in natural fluid inclusions are mathematically treated in the binary H_2O-NaCl system in most studies, to produce equivalent NaCl fractions that correspond to these temperatures in the binary H_2O-NaCl system despite the presence of other ions in the liquid solution. Second, a vapour phase must be present in order to interpret dissolution temperatures directly, but the properties of this phase are in general neglected, because both density and salinity are extremely low compared to the liquid phase (e.g. Chou, 1987; Diamond, 2003). Bakker (2011, 2012a) illustrated that the properties of the vapour phase become increasingly important for the estimation of the bulk fluid at higher salinities and temperatures.

According to standard thermodynamic principles, two parameters have to be quantified in binary fluid systems in order to calculate bulk fluid properties in inclusions (i.e. constant total volume), such as dissolution temperature of halite (T_m), homogenization temperature of liquid and vapour (T_h), volume fraction of the vapour phase (φ^{vap}) (e.g. Diamond, 2003). Temperatures of changes in phase assemblages are relatively easily determined by microthermometry, whereas volume fractions estimations require some effort (Bakker and Diamond, 2006). The development of phase assemblages in a heated fluid inclusion that contain halite, liquid, and vapour (*SLV*) at room temperatures is illustrated in a schematically isoplethic projection in Figure. 1 (c.f. Fig. 4 in Bakker, 2012a). Inclusions with lower density (isochore 2 in Fig. 1) reveal systematic higher dissolution temperatures (*SLV* → *LV*) than higher density inclusions (isochore 1 in Fig. 1), although both have the same bulk salinity. Bakker (2011, 2012a) quantified this effect by using the equation of state for binary H_2O-NaCl solution according to Anderko and Pitzer (1993a), in combination with a well-defined *SLV* curve (see Bakker, 2012b, and reference therein). This equation of state is mathematically restricted to temperatures above 300 ˚C. This thermodynamic model was used to design molar volume-composition (*Vx*) diagrams (Fig. 8 and 9 in Bakker, 2012a) with projections of equal T_h (*LV* → *L*) and equal T_m (*SLV* → *LV*) lines (Fig. 2a). In addition, the volume fraction of the vapour phase at T_m can be also selected to estimate bulk fluid properties in addition to T_m values (Fig. 2b). The measurement of two parameters gives directly bulk salinity and molar volume of a fluid inclusion within these diagrams.

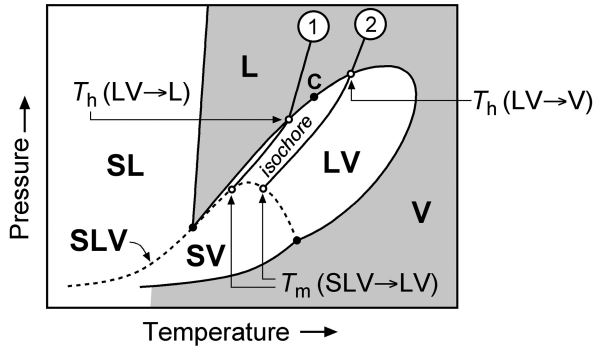

Fig. 1.
Schematical *p-T* diagram of the binary H_2O-NaCl system. Isochores are illustrated for a high-density fluid (1) that homogenize in the liquid phase, and a low-density fluid (2) that homogenize in the vapour phase. The isochores intersect with the *SLV* curve producing different T_m values for the same bulk salinity. The shaded area contains a homogeneous fluid, whereas the white area contains two phases, either *LV*, *SL* or *SV*. After Bakker (2012a). *C* is the critical point.

Steele-MacInnis and Bodnar (2013) addressed their research to the same topic as Bakker (2012a), to characterize also the effect of the vapour phase on the salinity estimation of halite-bearing aqueous inclusions. Their intention was to present purely empirical best-fit equations that may replace the above-mentioned *Vx* diagrams. The experimental approach in their work is inappropriate, it does not provide true experimental data, and it does not illustrate an estimate of uncertainty, accuracy and precision of the results. The mathematical modelling with purely empirical best-fit equations is insufficient, and partly erroneous. Comparison with the model from Bakker (2012a) results in highly incorrect, inconsistent and imprecise statements about the quality of the results from Bakker (2012a). Furthermore, the authors use "supplementary data" to continue this improper comparison with Bakker (2012a) in a discussion without peer-review. The following paragraphs will elucidate these comments.

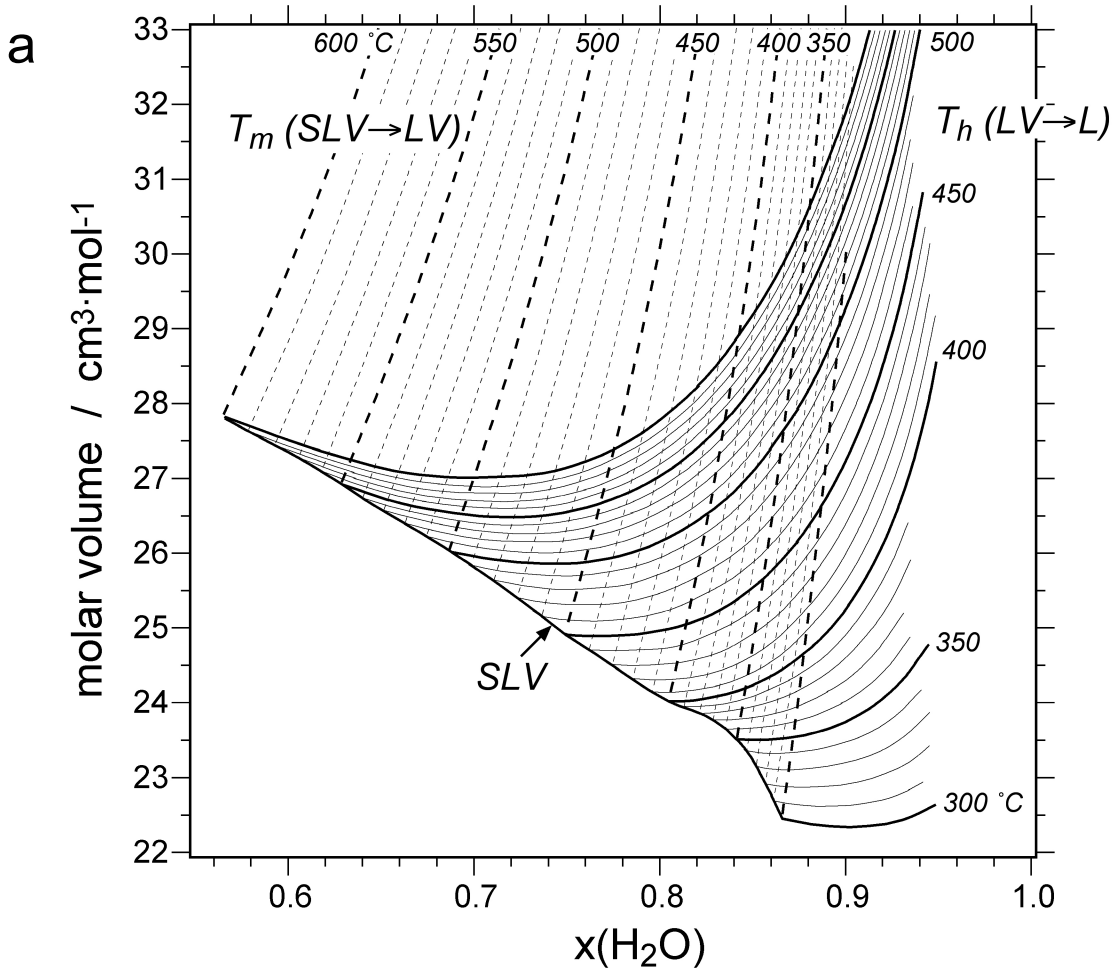

Fig. 2. *Vx* diagrams of the binary H_2O-NaCl system with (**a**). iso-T_h (solid lines) and iso-T_m lines (dashed lines); (**b**) iso-T_m (dashed lines) and iso-φ^{vap} lines (solid lines). After Bakker (2012a).

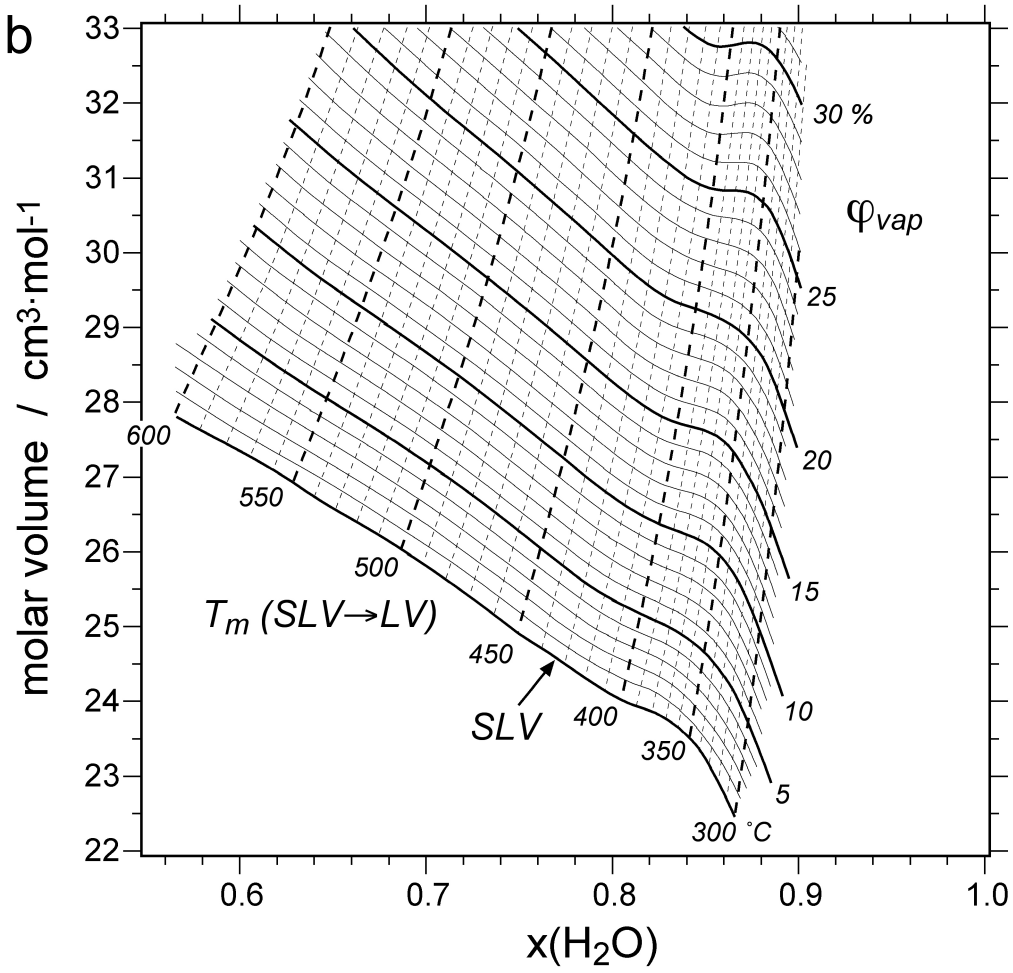

Fig. 2. *Continued*

2. SLV CURVE: EXPERIMENTAL METHOD AND RESULTS

Steele-MacInnis and Bodnar (2013) present results of experiments that repeat those of Sterner et al. (1988), to test the reproducibility and reliability of the properties of the *SLV* curve. The experimental method to synthesize highly saline fluid inclusions is based on loading separately known masses of H_2O and NaCl in capsules that also contain quartz cores with microcracks, which will subsequently heal at high temperatures and pressure and which will form numerous fluid inclusions that enclose a homogeneous brine (see Bodnar and Sterner, 1987). Crack-healing processes are instantaneously and may already occur during uploading and downloading of experiments, i.e. at temperatures and pressures that may differ from the intended experimental conditions. Moreover, crack healing may occur before the separate loaded phases homogenize in one highly saline liquid-like phase. Consequently, a variety of densities and salinities may occur in a fluid inclusion assemblage, although a majority may correspond to the intended conditions. Table 2 in Steele-MacInnis and Bodnar (2013) illustrates experimental conditions, average dissolution temperatures and average homogenization temperatures, but lacks uncertainty analyses. True experimental data are not presented in this manuscript and supplementary material. The average values are based on the measurements of an undefined number of fluid inclusions (5 to 15). Steele-MacInnis and Bodnar (2013) indicate that they measured a variation of 0.5 ˚C in T_m (*SLV*→*LV*) and 5 ˚C variation in T_h (*LV*→*L*), and classify this variation as a normal range which is irrelevant to the accuracy of the results. Variations in temperatures are regarded as "random errors" which do not exceed ± 1 ˚C (Steele-MacInnis and Bodnar, 2013), however these numbers highly underestimate the illustrated variation in homogenization temperatures. Experimental work in our laboratory has revealed a much larger variation in dissolution temperatures of halite if a larger population of highly saline synthetic fluid inclusions is taken into account. This is consistent with the experimental work from Sterner et al. (1988), and can be deduced from their Table 1 (Fig. 3). The variation is about 3 ˚C if only 8 inclusions are measured, whereas a variation of 30 ˚C is reached if at least 25 inclusions are measured. The experimental technique and the experimental laboratory used by Sterner et al. (1988) and those used by Steele-MacInnis and Bodnar (2013) are the same. Therefore, the variation and uncertainty must be similar to that of Sterner et al. (1988), although this information cannot be deduced from Steele-MacInnis and Bodnar (2013). Consequently, the presented

average values in Table 2 cannot be scrutinized on reliability, and do not contribute to a better understanding of the *SLV* curve in binary H_2O-NaCl solutions, and the interpretation of natural fluid inclusions. A larger variation in microthermometric data is suggested in paragraph 3.1 in Steele-MacInnis and Bodnar (2013) by mentioning that they selected only "eight synthetic fluid inclusion samples that showed < 50 ˚C difference ...".

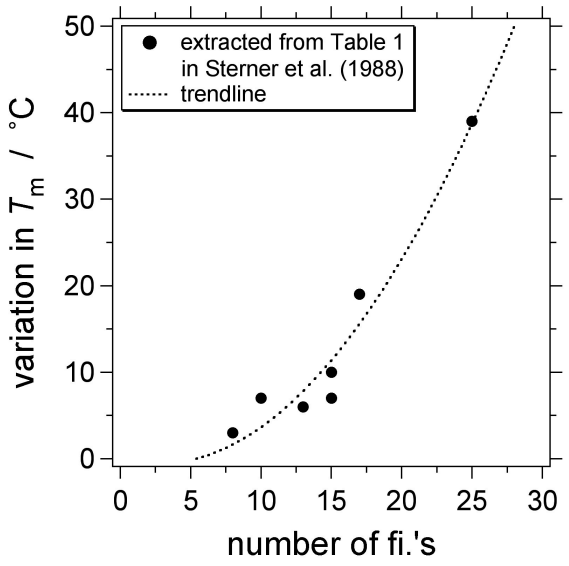

Fig. 3. Variation in T_m values in binary H_2O-NaCl-rich inclusions as a function of the number fluid inclusions measured in one sample, according to the experimental data from Sterner et al. (1988).

The volumetric properties (φ^{vap}) of these inclusions at T_m were only approximately analyzed in Steele-MacInnis and Bodnar (2013) by comparison with the appearance diagram of hypothetical spherical and flat circular fluid inclusions (Roedder, 1984). Bakker and Diamond (2006) have already illustrated that this approximate method is highly inaccurate, and can be greatly improved by using a spindle stage and two-dimensional images of a specific fluid inclusion.

3. EFFECT OF THE VAPOUR PHASE: EXPERIMENTAL METHOD AND RESULTS

The experimental work from Bodnar (1994) illustrated microthermometric data for fluid inclusions with a 40 mass% NaCl solution, which homogenize by vapour phase disappearance (Table 2 in Bodnar, 1994), in addition to the main topic of this work, i.e. determination of the liquidus (*SL* → *L* curve). Similar to Table 2 and 3 in Steele-MacInnis and Bodnar (2013), only average values are given, and the lack of true experimental data does not allow an estimation of the uncertainty and reliability of these numbers. Steele-MacInnis and Bodnar (2013) used the "bracketing approach" to overcome difficulties in loading an exact composition into capsules before experimentation. Each experiment was performed twice, with a slightly higher and lower concentration of NaCl. Table 3 in Steele-MacInnis and Bodnar (2013) does not provide verifiable results and information about both types of experiments, but gives an average value of dissolution and homogenization temperatures without an indication of any variation and without the number of inclusions that are measured. This experimental method result in a variety of factors that increase the uncertainty and reliability, in addition to the factors already mentioned in the previous paragraph.

Most of the experiments presented in Table 3 in Steele-MacInnis and Bodnar (2013) are performed within the β-quartz stability field. The effect of the α–β phase change in quartz on the properties of fluid inclusions has not yet been systematically studied, although in each experiment this boundary is crossed twice. Decrepitation experiments at room pressures (e.g. Hladky and Wilkins, 1990) clearly indicate a "peak noise" at the α–β phase change (≈ 572 ˚C) that may correspond to a massive irreversible decrepitation of all fluid inclusions in a quartz sample. Recent experiments by Doppler et al. (2013, and 2014) have indicated that fluid inclusions are affected by the α–β phase change at higher experimental temperatures and pressures.

A discussion about the results of the contribution of the vapour phase to bulk salinity in fluid inclusions is already given in paragraph 3.3 in Steele-MacInnis and Bodnar (2013). It is suggested that this contribution is related to density of the vapour phase along the *SLV* curve, which is maximized at higher pressures along this curve (between 500 and 600 ˚C). However, a substantial different but correct statement is: divergence of bulk salinity determined by dissolution temperature only (e.g. Sterner et al., 1988) and determined by both homogenization and dissolution temperatures (Figure 8 and 9 in Bakker, 2012a) systematically increase with higher temperatures and higher bulk salinities.

4. MATHEMATICAL MODELLING AND COMPUTER PROGRAMS

Purely empirical model of binary H_2O-NaCl solution according to Driesner and Heinrich (2007) and Driesner (2007) can be applied to predict all the fluid properties in the experimental work from Steele-MacInnis and Bodnar (2013). For example, Driesner and Heinrich (2007) and Driesner (2007) define clear boundary conditions for purely empirical equations that allow a complete interpretation of the H_2O-NaCl system along the *SLV* curve. However, Steele-MacInnis and Bodnar (2013) prefer to use new purely empirical fits of liquid and vapour density along the *SLV* curve (based on tabled values in Driesner and Heinrich, 2007), and they prefer to use the correlation from Sterner et al. (1988) to calculate the salinity along the *SLV* curve. The purely empirical fitting in Steele-MacInnis and Bodnar (2013) is based on a simple polynomial fitting of parameters, without the natural limitation of phase boundaries, and it results, therefore, occasionally in highly inaccurate numbers. Moreover, a purely empirical fit to numbers resulting from the model of Driesner and Heinrich (2007) is in principle a double fitting procedure, that result in less accurate numbers if the complexity of the second fitting equation is less than the first.

The mathematical approach in Steele-MacInnis and Bodnar (2013) compares bulk densities that are estimated at T_m (at an arbitrary selected salinity) with bulk densities that are estimated at T_h by using Eq. 1 (in Steele-MacInnis and Bodnar, 2013). It is claimed that this equation calculates the density of a liquid phase throughout the region of liquid-vapour coexistence (see *LV* in Fig.1), independent of pressure. However, this equation can only reproduce liquid densities at the *SLV* curve (c.f. Driesner, 2007). Consequently, the mathematical approach, as illustrated in Fig.3 in Steele-MacInnis and Bodnar (2013), must result in erroneous numbers.

A third stage of purely empirical fitting is applied in Eq. 3 in Steele-MacInnis and Bodnar (2013), that relates directly the volume fraction of liquid (φ^{liq}) at T_m with dissolution and homogenization temperatures. The parameters involved in this stage are obtained from the previously mentioned mathematical approach. It must be noted that the uncertainty and reliability of numbers increase in each additional stage of purely empirical fitting procedures.

The combination of Eqs. 1, 2, and 3 in Steele-MacInnis and Bodnar (2013) results in an "easy-to-use" method that can be incorporated in simple spreadsheet-based programs, unlike highly complex thermodynamic models. The reliability of these equations is highly questionable according to the previously mentioned considerations, and the application of simple equations is always limited within thermodynamics. They usually cannot be used to predict the fluid properties of an entire fluid system, and may lead to highly inaccurate numbers if boundary conditions are not well defined.

Software that includes highly complex thermodynamic models, and also purely empirical models to calculate the properties of binary H_2O-NaCl solutions are included in the package "*FLUIDS*" (Bakker, 2003; Bakker and Brown, 2003). This package is continuously updated with additional programs (e.g. Bakker, 2009; Bakker, 2012b; Bakker, 2012c; all programs are downloadable for Macintosh and Windows operating systems at http://fluids.unileoben.ac.at) for an increased number of equations of state for fluids, to make complex mathematical procedure available and easy-to-use to all fluid inclusion researchers. This software was used to calculate fluid inclusion properties from T_m and T_h values in Bakker (2012a), but is completely ignored by Steele-MacInnis and Bodnar (2013). The programs "*AqSoWNK*" (Bakker, 2012b) and "*LonerAP*" (http://fluids.unileoben.ac.at) can be combined to calculate the properties of binary NaCl-H_2O fluids along the *SLV* curve, whereas "*LonerAP*" can be used to calculate homogenization conditions in the *LV* field above 300 ˚C. These programs contain a large variety of calculation possibilities that can be applied to multiple research interests. A new program is designed, "*AqSoDH*" (available at http://fluids.unileoben.ac.at) to handle binary NaCl-H_2O fluids from the purely empirical model according to Driesner and Heinrich (2007) and Driesner (2007), that can be applied to the entire H_2O-NaCl system between 0 and 1000 ˚C, 0.1 and 500 MPa, and 0 to 1 x(NaCl).

5. *VX* DIAGRAM

A molar volume-composition (*Vx*) diagram of the binary H_2O-NaCl system (Fig. 2) was designed by Bakker (2012a) using the thermodynamic model of Anderko and Pitzer (1993a) and a well-defined *SLV* curve (Bakker, 2012b, and references therein). The advantage of these type of diagrams in fluid inclusion research was already illustrated by Burruss (1981) and Thiéry et al. (1994), but found only little attention in literature. The desired parameters, i.e. bulk composition and molar volume of fluid inclusions are directly obtained from the intersection of projected equal T_h and equal T_m curves (or equal φ^{vap} curves). The values are obtained from a graphical interpretation of these types of phase diagrams, which is not difficult to apply in practise. In other words, one plots the measured temperatures and reads off the true salinity and molar volume directly. Bakker (2012a) mentioned that the use of software "Datathief" (Tummers, 2006) increases the precision of extracted *Vx* data points in scanned diagrams.

The *Vx* diagram of the binary H_2O-NaCl system from Bakker (2012a) is argued by Steele-MacInnis and Bodnar (2013) in paragraph 4.2 to include conditions that are not relevant to fluid inclusion studies. First, homogenization temperatures are not included in the *Vx* diagram of Figure 9 in Bakker (2012a), because they would exceed the limits of heating stages, but volume fraction of the vapour bubble is selected instead as a second constraint in this fluid system. Second, the considerations of Steele-MacInnis and Bodnar (2013) exclude the possibility to entrap

a vapour-like fluid at higher temperature and pressure, because homogenization conditions would exceed the stability conditions of the minerals. In addition, they proclaim that heterogeneous trapping does not give information about trapping condition of fluid inclusions (paragraph 4.2 in Steele-MacInnis and Bodnar, 2013). These are major mistakes in understanding trapping conditions of fluid inclusions, and possible post-entrapment modifications of fluid inclusions. It is general knowledge that trapping conditions can be directly obtained from homogenization conditions of coexisting liquid-rich and vapour-rich fluid inclusions (e.g. Shepherd et al., 1985; Diamond, 2003). The occurrence of heterogeneous trapping in nature is more common than illustrated in most fluid inclusion research, because the presence of multiple components in a pore fluid system (e.g. a variety of dissolved salts) result in a huge fluid-immiscibility field up to high temperatures and pressures. The phase diagram illustrated in Fig.9 in Bakker (2012a) is not "misleading" (paragraph 4.2 in Steele-MacInnis and Bodnar, 2013) but illustrates fluid properties in a wide range of conditions according to the equation of state from Anderko and Pitzer (1993a). Natural fluid conditions cannot be deduced from this diagram, but it includes all possible fluid properties that can be calculated with this equation of state, either at experimental laboratory conditions or in natural rock.

The equation of state from Anderko and Pitzer (1993a and 1993b) (program "*Loner AP*", http://fluids.unileoben.ac.at) can be used to illustrate heterogeneous trapping of a hypothetical natural fluid with 50 mass% NaCl, x(NaCl) = 0.2356. This fluid is immiscible in a closed system below homogenization conditions at 1000 ˚C and 261.6 MPa. The bulk molar volume of this fluid is 33.15 $cm^3 \cdot mol^{-1}$ (0.8310 $g \cdot cm^{-3}$). At 990 ˚C and 251.7 MPa, this fluid is unmixed in a liquid phase (33.18 $cm^3 \cdot mol^{-1}$, x(NaCl) = 0.2362) and a vapour phase (37.46 $cm^3 \cdot mol^{-1}$, x(NaCl) = 0.1170). Both fluids can be entrapped in fluid inclusions that are formed under these conditions, and both type of fluid inclusions have the same total homogenization temperature. At room temperature, both types of fluid inclusions contain three phase, i.e. halite, brine and vapour (*SLV*). Dissolution temperatures of halite can be measured in both types. The lower molar volume type reveals a dissolution temperature of 445 ˚C, in the presence of a brine (24.87 $cm^3 \cdot mol^{-1}$, x(NaCl) = 0.2506, φ^{liq} = 0.7051) and a vapour (162.60 $cm^3 \cdot mol^{-1}$, x(NaCl) = 0.00009, φ^{vap} = 0.2949). The temperature limit of most heating stages does not allow the measurement of total homogenization ($LV \rightarrow L$), therefore, the volume fraction can be used in addition to dissolution temperatures to estimate bulk fluid properties in these inclusions (see Bakker, 2012a). The calculated values are consistent with the purely empirical model from Driesner and Heinrich (2007) and Driesner (2007), and cannot be estimated with the model from Steele-MacInnis and Bodnar (2013). Unlike the statements in paragraph 4.2 of Steele-MacInnis and Bodnar (2013), these conditions (i.e. high temperature and relative low pressures) do occur in natural rock, without the formation of a melt.

6. COMPARISON BETWEEN MODELS AND EXPERIMENTAL DATA

An objective comparison with thermodynamic models (e.g. Anderko and Pitzer, 1993a; Bakker, 2012) and purely empirical models (Driesner and Heinrich, 2007; Driesner, 2007) is not given in the paper of Steele-MacInnis and Bodnar (2013). Moreover, experimental data other than their fluid inclusion data are not used in this study to illustrate the accuracy of their model. A contradiction in statements about the accuracy of the model according to Bakker (2012a) is given in paragraph 3 in Steele-MacInnis and Bodnar (2013) where they describe the consistency between their data, the modelling from Bakker (2012a) and the consideration from Chou (1987), and paragraph 4 where they describe a "systematically inconsistent" liquid salinity along the *SLV* curve according to Bakker (2012a). The latter is further discusses in the appendix (see "supplementary data", Steele-MacInnis and Bodnar, 2013), which does not contain complementary data, such as extended data sets, or a more detailed description of the method, but is composed of an unreviewed discussion about the results from Bakker (2012a). Moreover, it contains a *Vx* diagram without tick marks that cannot be used or directly compared with other *Vx* diagrams such as presented in Bakker (2012a).

A comparison of the liquid salinity, liquid density, and vapour density along the *SLV* curve between the models of Driesner and Heinrich (2007), Bakker (2012a) and Steele-MacInnis and Bodnar (2013) is illustrated in Tables 1, 2, and 3, respectively. The liquid salinity according to Anderko and Pitzer (1993a) and Bakker (2012a) is locally lower than the values calculated with the other models (Table 1), as numerously pointed out by Steele-MacInnis and Bodnar (2013). It must be noted that the uncertainties in salinity values are determined by the variation in T_m values in synthetic fluid inclusions, as illustrated by Sterner et al. (1988). A variation of 2.6 and 5.3 mass% can be deduced directly from T_m variations in Table 1 from Sterner et al. (1988) at experimentally intended compositions of 62.4 and 80 mass%, respectively. This variation becomes smaller at lower salinities, but, as mentioned before, this variation depends on the number of inclusions measured (Fig. 3). Consequently, all calculated numbers in Table 1 are within the limits of this uncertainty. Furthermore, there are no substantial differences in liquid and vapour phase densities along the *SLV* curve (Tables 2 and 3, respectively), except that the liquid density according to Steele-MacInnis and Bodnar (2013) is increasingly deviating at higher temperatures (at 790 and 800 ˚C in Table 2).

Driesner and Heinrich (2007) concluded from a comparison of experimental data that the composition of the saturated liquid on the *SLV* surface is well characterized at low temperatures, but there is substantial disagreement in the high temperature range. The vapour composition along the *SLV* curve is not well known, except for intermediate temperatures. The uncertainties and incomplete fluid inclusion data do not improve the accuracy of these purely empirical models.

Table 1. Calculated NaCl mass% of the liquid phase along the *SLV* curve

Temperature ˚C	Bakker (2012a) Anderko and Pitzer (1993a)	Driesner and Heinrich (2007)	Sterner et al. (1988)
310	35.9	38.5	38.9
400	46.6	47.1	47.4
500	59.6	59.9	59.7
600	71.8	74.2	73.8
700	85.1	88.0	87.5
790	98.6	98.8	98.0
800	100.0	99.9	99.1

Table 2. Calculated molar volume (in $cm^3 \cdot mol^{-1}$) of liquid phase along the *SLV* curve

Temperature ˚C	Bakker (2012a) Anderko and Pitzer (1993a)	Driesner (2007)	Steele-MacInnis and Bodnar (2013)
310	22.8	22.5	22.6
400	24.3	24.3	24.5
500	25.9	26.4	26.5
600	27.9	28.7	28.6
700	31.3	32.1	31.7
790	36.6	36.9	35.8
800	37.4	37.6	36.4

Table 3. Calculated molar volume (in $cm^3 \cdot mol^{-1}$) of vapour phase along the *SLV* curve

Temperature ˚C	Bakker (2012a) Anderko and Pitzer (1993a)	Driesner (2007)	Steele-MacInnis and Bodnar (2013)
310	580.3	565.3	561.4
400	202.5	222.0	222.8
500	139.4	140.9	141.1
600	147.5	149.9	150.3
700	256.5	261.1	259.6
790	2289.6	2372.5	2300.2
800	11361.6	36164.8	13929.8

7. ADVANTAGE OF THERMODYNAMIC MODELLING

Fundamental thermodynamic principles account for all the phenomena that can be observed in fluid inclusions, and they regulate the appearance of purely empirical mathematical equations that mirrors the relationship between thermodynamic parameters within a relative small range of conditions. These principles can be applied to the entire binary H_2O-NaCl system, but are completely ignored in the considerations of Steele-MacInnis and Bodnar (2013). A major advantage of thermodynamic modelling is that it may include more fluid components, such as KCl (Anderko and Pitzer, 1993b), CO_2 (Duan et al., 1995) and CH_4 (Duan et al., 2003), whereas purely empirical equations are highly restricted to only a small part of the available data in the binary H_2O-NaCl system. Thermodynamical modelling is, therefore, more reliable for the analysis of natural fluid inclusion systems, that usually contain a large variety of components.

REFERENCES

Anderko A. and Pitzer K. S. (1993a) Equation-of-state representation of phase equilibria and volumetric properties of the system NaCl-H_2O above 573 K. *Geochim. Cosmochim. Acta* **57**, 1657-1680

Anderko A. and Pitzer K. S. (1993b) Phase equilibria and volumetric properties of the systems KCl-H_2O and NaCl-KCl-H_2O above 573 K: Equation of state representation. *Geochim. Cosmochim. Acta* **57**, 4885-4897.

Bakker R. J. (2003) Package FLUIDS. Part 1: Computer programs for analysis of fluid inclusion data and for modelling bulk fluid properties. *Chem. Geol.* **194**, 3-23.

Bakker R. J. (2009) Package FLUIDS. Part 3: Correlations between equations of state, thermodynamics and fluid inclusions. *Geofluids* **9**, 63-74.

Bakker R. J. (2011) The relationship between salinity, dissolution temperature of halite and volume fraction of the vapour phase in the binary H_2O-NaCl system. In *ECROFI XXI abstracts* (eds. R. J. Bakker, M. Baumgartner and G. Doppler) *Ber. Geol. Bund*. **87**, 34-35.

Bakker R. J. (2012a) Can the vapour phase be neglected to estimate bulk salinity of halite bearing aqueous fluid inclusions. *Cent. Eur. J. Geosci*. **4**, 238-245.

Bakker R. J. (2012b) Package FLUIDS. Part 4: Thermodynamic modelling and purely empirical equation of state for H_2O-NaCl-KCl solutions. *Mineral. Petrol.* **105**, 1-29

Bakker R. J. (2012c) Thermodynamic properties and applications of modified van-der-Waals equations of state. In *Thermodynamics - Fundamentals and its Application in Science* (ed. R. Morales-Rodriguez), InTech, Croatia, pp. 163-190.

Bakker R. J. and Brown P. E. (2003) Computer modelling in fluid inclusion research. In *Fluid Inclusions, Analysis and Interpretation* (eds. I. Samson, A. Anderson and D. Marschall) Short course 32, Mineralogical Association of Canada, Ottowa, pp. 175-212.

Bakker R. J. and Diamond L. W. (2006) Estimation of volume fractions of liquid and vapour phases in fluid inclusions, and definition of inclusion shape. *Am. Mineral.* **91**, 635-657.

Bodnar R. J. (1994) Synthetic fluid inclusions. XII. The system H_2O-NaCl. Experimental determination of the halite liquidus and isochores for a 40 wt.% NaCl solution. *Geochim. Cosmochim. Acta* **58**, 1053-1063.

Bodnar R. J. and Sterner S. M. (1987) Synthetic fluid inclusions. In *Hydrothermal Experimental Techniques* (eds, G. C. Ulmer and H. L. Barnes). Wiley-Interscience, New York, pp. 423-457.

Burruss R. C. (1981) Analysis of phase equilibria in C-O-H-S fluid inclusions. In *Fluid inclusions: applications to petrology* (eds. L. S. Hollister and M. L. Crawford) Short course 6, Mineralogical Association of Canada, pp. 39-74.

Chou I.-M. (1987) Phase relations in the system NaCl-KCl-H_2O. III. Solubilities of halite in vapor-saturated liquids above 445 ˚C and redetermination of phase equilibrium properties in the system NaCl-H_2O to 1000˚C and 1500 bars. *Geochim. Cosmochim. Acta* **51**, 1965-1975.

Diamond L. W. (2003) Introduction to gas-bearing, aqueous fluid inclusions. In *Fluid Inclusions, Analysis and Interpretation* (eds. I. Samson, A. Anderson and D. Marschall) Short course 32, Mineralogical Association of Canada, Ottowa, pp. 101.158.

Doppler G., Bakker R. J. and Baumgartner M. (2013) The effect of α-β-quartz transition boundary in re-equilibration experiments. In *ECROFI XXII, Abstract book* (eds. N. Hanilci and G. Bozkaya) Turkey, pp. 12-14.

Doppler G., Bakker R. J. and Baumgartner M. (2014) The effect of α-β-quartz transition of quartz on fluid inclusions during re-equilibration experiments. *Lithos* **198-199**, 4-23.

Driesner T. (2007) The system H_2O-NaCl. Part II: Correlations for molar volume, enthalpy, and isobaric heat capacity from 0 to 1000 ˚C, 1 to 5000 bar, and 0 to 1 X_{NaCl}. *Geochim. Cosmochim. Acta* **71**, 4902-4919.

Driesner T. and Heinrich C. A. (2007) The system H_2O-NaCl. Part I. Correlation formulae for phase relations in temperature-pressure-composition space from 0 to 1000 ˚C, 0 to 5000 bar, and 0 to 1 X_{NaCl}. *Geochim. Cosmochim. Acta* **71**, 4880-4901.

Duan Z., Møller N. and Weare J. H. (1995) Equation of state for the NaCl-H_2O-CO_2 system: Prediction of phase equilibria and volumetric properties. *Geochim. Cosmochim. Acta* **59**, 2869-2882.

Duan Z., Møller N. and Weare J. H. (2003) Equation of state for the NaCl-H_2O-CH_4 system and the NaCl-H_2O-CO_2-CH_4 system: Phase equilibria and volumetric properties above 573 K. *Geochim. Cosmochim. Acta* **67**, 671-680.

Hladky G. and Wilkins R. W. T. (1987) A new approach to fluid inclusion decrepitometry - practice. *Chem. Geol.* **61**, 37-45.

Roedder E. (1984) *Fluid Inclusions, Reviews in Mineralogy 12*. Mineralogical Society of America, Washington DC.

Shepherd T. J., Rankin A. H. and Alderton D. H. M. (1985) *A practical guide to fluid inclusion studies.* Blackie, Glasgow.

Steele-MacInnis M. and Bodnar R. J. (2013) Effect of the vapour phase on the stability of halite-bearing aqueous fluid inclusions estimated from the halite dissolution temperature. *Geochim. Cosmochim. Acta* **115**, 205-216.

Sterner S. M., Hall D. L. and Bodnar R. J. (1988) Synthetic fluid inclusions. V. Solubility relations in the system NaCl-KCl-H_2O under vapor-saturated conditions. *Geochim. Cosmochim. Acta* **52**, 989-1006.

Thiéry R., van den Kerkhof A. M. and Dubessy J. (1994) vX properties of CH_4-CO_2 and CO_2-N_2 fluid inclusions: modelling for T < 31 ˚C and P < 400 bars. *Eur. J. Mineral*. **6**, 753-771.
Tummers B. (2006) *DataThief III*, http://datathief.org.